

1 **Chemical thermodynamics and kinetics of thiophenic sulfur removed**
2 **from coal by microwave: A density functional theory study**

3 Chen Yin¹, Shengfu Zhang^{1,2,*}, Jincheng Wang¹, Farooq Sher³, Shuangshuang Cai¹, Jian Xu¹,
4 Meilong Hu¹, Liangying Wen¹

5 ¹College of Materials Science & Engineering, Chongqing University, Chongqing 400044, P.R. China

6 ²Chongqing Key Laboratory of Vanadium-Titanium Metallurgy & Advanced Materials, Chongqing
7 University, Chongqing 400044, P.R. China

8 ³ Department of Engineering, School of Science and Technology, Nottingham Trent University,
9 Nottingham NG11 8NS, UK

10 Chen Yin, E-mail: yinchen@cqu.edu.cn

11 *Shengfu Zhang (Corresponding author), E-mail: zhangsf@cqu.edu.cn

12 Jincheng Wang, E-mail: wjc17307406593@163.com

13 Farooq Sher, E-mail: Farooq.Sher@ntu.ac.uk

14 Shuangshuang Cai, E-mail: 201809131196@cqu.edu.cn

15 Jian Xu, E-mail: jxu@cqu.edu.cn

16 Meilong Hu, E-mail: hml@cqu.edu.cn

17 Liangying Wen, E-mail: cquwen@cqu.edu.cn

18

19 **Abstract**

20 In this study, the feasibility of catalyzing removal of thiophenic sulfur from coal with microwave
21 irradiation was evaluated by dielectric properties test, and the chemical thermodynamics and kinetics of
22 thiophenic sulfur in coal with microwave irradiation was obtained by density functional theory
23 calculation. Results suggested that the imaginary parts of dielectric constants ϵ'' of benzothiophene and
24 dibenzothiophene are higher than those of coal samples, meaning that thiophenic sulfur compounds in
25 the coal can be selectively heated by microwave. Linear Synchronous Transit/Quadratic Synchronous
26 Transit method indicated that the microwave field catalyzed the removal of thiophenic sulfur mainly
27 affected the breaking of C–H and C–C bonds, thus reducing the energy barrier (E_b) and activation energy
28 (E_a) and increasing the logarithm of rate constants ($\ln k$) in the desulfurization process. Moreover, the
29 optimal removal path of thiophenic sulfur changed from $\beta(a)$ to $\alpha(b)$, and sulfur-containing products
30 changed from carbon monosulfide (CS) to thioketene(C_2H_2S) after applied microwave field. These
31 findings reveal the catalytic mechanism of microwave on the removal of thiophenic sulfur in coal from
32 hydrogen migration and reaction changes, which is conducive to the clean utilization of coal.

33 **Keywords:** Thiophenic sulfur; Microwave; Dielectric properties; Coal desulfurization; DFT.

34

35 **1. Introduction**

36 In a long period of time in the future, blast furnace will still be the leading process of molten iron
37 production. According to statistics [1], the molten iron production of blast furnace in China was about

38 8.88×10^8 t in 2020. Based on the coke ratio of $350 \text{ kg} \cdot \text{t}^{-1}$, the consumption of high-quality coking coal in
39 China's metallurgical industry reached 5.0×10^8 t in 2020. Due to excessive development and
40 consumption, the supply of high-quality coking coal with low ash and sulfur content have exceeded
41 demand in recent years, and the coke price has increased by nearly 10% year on year [2-6]. As we know,
42 for metallurgical industry, the direct utilization of high sulfur coal will not only produce SO_2 , H_2S , COS
43 and other gases, leading to extremely environment pollute and equipment corrosion, but also reduces the
44 quality of coke and molten iron [2, 7-10]. Therefore, it is crucial important to remove sulfur from high
45 sulfur coking coal to meet the resource allocation and realize the sustainable development of
46 metallurgical industry [11-13].

47 The main existing form of sulfur in coal is inorganic sulfur and organic sulfur [14]. Some relative
48 studies pointed out that the inorganic sulfur is mainly pyrite and sulfate, and it is mostly contained in coal
49 in the form of fine particles [15], can be removed by physical and chemical methods [15-20]. The organic
50 sulfur is a part of macromolecular structure of coal, including thiols, thioether, thiophene, etc. [21, 22].
51 Tang et al. [23] used peracetic acid to remove sulfur from coal, the removal rate of organic sulfur was
52 49%, this method would destroy the coal matrix while removing the organic sulfur. Results of these
53 studies showed that it is very difficult to remove organic sulfur in coal desulfurization [24-29].

54 Microwave desulfurization is a novel coal desulfurization method, can selectively and rapidly heat
55 sulfur components in coal [17]. The results show that microwave can accelerate the desulfurization
56 reaction of coal without destroying the coal matrix, and has great application potential for the removal

57 of organic sulfur such as thiol, thioether and thiophenic sulfur in coal [30-35]. Under microwave
58 irradiation, the removal of organic sulfur functional groups in coal is achieved by the dissociation of C–
59 S bonds, and the degree of difficulty of its fracture is related to the dielectric properties of sulfur-
60 containing substances. Previous studies have shown that the thioether in coal is easily oxidized to the
61 corresponding sulfoxide or sulfone under microwave conditions, while the C-S bond in thiophene and
62 thiophenone is difficult to break [36]. This is consistent with our previous studies, thiophenic sulfur
63 accounted for more than 60% of the total organic sulfur, but the removal rate was the lowest among the
64 three functional groups, only 18.9% [33]. These results indicate that the removal of thiophenic sulfur is
65 the key to coal desulfurization. However, previous studies have focused more on the removal of thiol and
66 thioether sulfur, and less analysis on the dielectric properties and removal mechanism of thiophenic sulfur.

67 The aim of this research was to clarify the dielectric property of thiophenic sulfur and mechanism
68 of bond-breaking removal with microwave irradiation. Agilent N5244A network analyzer has been used
69 to unravel the differences in dielectric properties between coal samples and thiophenic sulfur compounds.
70 Using the Materials Studio package, the Linear Synchronous Transit/Quadratic Synchronous Transit
71 (LST / QST) transition state search calculation of thiophenic sulfur in coal was carried out. The energy
72 barrier curve and activation energy of thiophene hydrogen migration and pyrolysis under microwave
73 electric field was obtained. The influence of microwave electric field on the thermodynamic and kinetic
74 parameters of the sulfur-containing model compound was explored.

75 2 Experimental

76 2.1 Samples preparation

77 Two typical high-sulfur coking coals (NTC and LGC) with different coal ranks, sulfur contents and
78 sulfur forms were selected as the study objection. **Table 1** presents the proximate, ultimate and sulfur
79 form analysis of the coal samples. The sulfur contents of NTC and LGC were 2.83% and 2.99% on dry
80 basis respectively, while the sulfur forms were significantly different. The organic sulfur content in NTC
81 is much higher than LGC, accounting for 87.99% of the total sulfur. Considerable pyrite sulfur and sulfate
82 sulfur occurs in LGC, which are 29.43% and 21.74% respectively. There is little difference in ash content
83 between the two coals, hardly effecting their dielectric properties.

84 In addition, the two types of thiophenic sulfur compounds, thiophene and benzothiophene, used in
85 this experiment were purchased from Bide Pharmatech Ltd., with a purity of 98%.

86

87

Table 1. Proximate, ultimate and sulfur form analysis of NTC and LGC

	Mass %	NTC	LGC
Proximate analysis	Moisture (air dry basis)	1.24	1.86
	Ash (dry basis)	10.37	8.46
	Volatile matter (dry basis)	17.92	30.11
	Fixed carbon (dry basis)	71.71	61.43
Ultimate analysis (dry basis)	C	87.62	84.67
	H	4.48	5.15
	N	1.39	1.42
	O	3.68	5.76
	S	2.83	2.99
Sulfur form analysis (dry basis)	Pyritic sulfur	10.60	29.43
	Sulfate sulfur	1.41	21.74
	Organic sulfur	87.99	48.83

88

89 **2.2 Dielectric property test**

90 A vector network analyzer was used to measure the dielectric constants of coal samples and
91 thiophenic sulfur compounds by the transmission reflection method [35]. Before measurement test, each
92 of samples dried were crushed and ground to a particle size less than 250 μm , then pressed into a circular
93 cylindrical sample with 7 ± 0.2 mm length, 3.04 mm inner diameter, and approximately 5.0 mm thickness.
94 The dielectric constant ε_0 and permeability μ_0 were measured at 2-10 GHz frequency range according
95 to Eq. (1) and (2) in reference [37].

$$96 \quad \varepsilon_0 = \varepsilon' + \varepsilon'' \cdot i \quad (1)$$

$$97 \quad \mu_0 = \mu' + \mu'' \cdot i \quad (2)$$

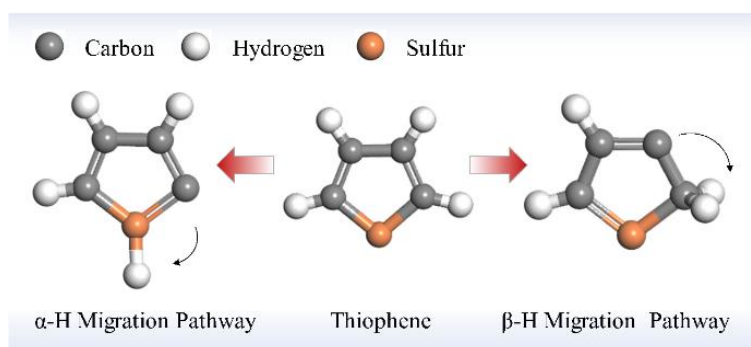
98 where ε' represents the dielectric constant real part, and the larger the value, the stronger the ability of
99 sample to store electric field energy. ε'' represents the dielectric constant imaginary part, and the larger
100 the value, the greater the ability of the sample to absorb electric field energy and convert it into heat
101 energy. The meaning of μ' and μ'' are similar with ε' and ε'' respectively. The higher the value of ε''
102 and μ'' , the more effective the microwave on the reaction.

103 **2.3 Density functional theory (DFT) calculation**

104 Thiophene is a common aromatic compound containing thiophenic sulfur in coal, which conforms
105 to Schucker rule ($4N + 2$). Compared with thiols and thioethers, the removal of thiophenic sulfur involves
106 not only the formation and breaking of chemical bonds, but also the transfer of H within the molecule.

107 The thiophenic sulfur migration path varies with the hydrogen migration path, so hydrogen migration
108 has been studied to reveal the catalytic effect of microwave on thiophene sulfur removal. According to
109 the previous studies [38-40], the following reaction paths with hydrogen transfer process (α -H migration
110 and β -H migration) were selected for the transition state search calculation, as shown in Fig. 1.

111



112

113 **Fig. 1. Diagram of thiophenic hydrogen migration pathway during desulfurization.**

114

115 All calculations were conducted by the Dmol³ modules [7] of Materials Studio package (version
116 6.0). In the process of finding the transition state by conjugate gradient method (CG) and LST/QST, the
117 key parameters were set as follows: Using GGA method with Perdew-Burke-Ernzerh of functional (PBE)
118 with DND basis set, and the optimal convergence was obtained. The threshold value was the combination
119 of medium parameters: the energy convergence was 2.0×10^{-5} Ha, the energy gradient was 1.00×10^{-3}
120 (Ha·bohr⁻¹), the displacement was 1.00×10^{-3} (Bohr), the spin multiplicity was octupole, the numerical
121 integration accuracy and SCF convergence control was medium, and the electric field was set at (0 0
122 0.01) au [39-41].

123 **3. Results and discussion**

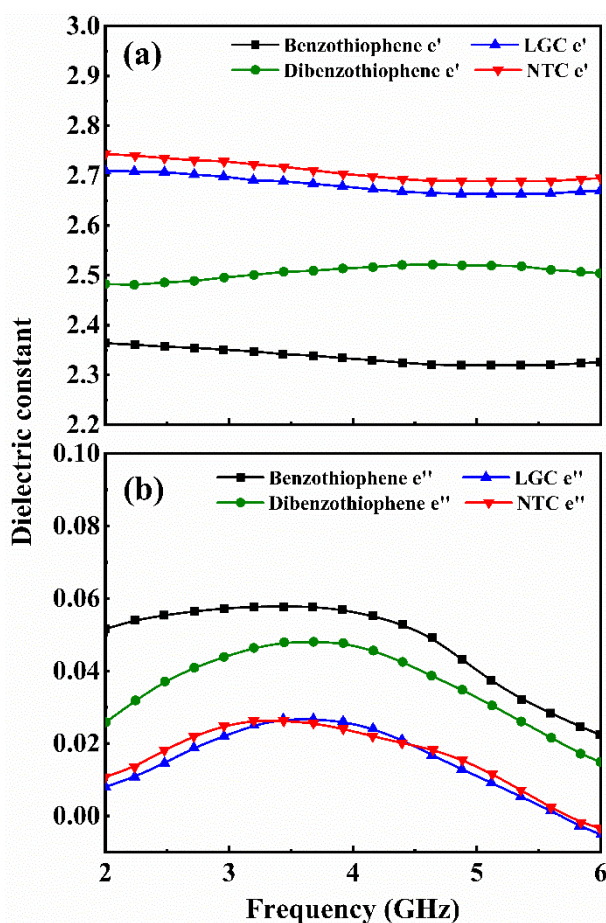
124 **3.1 Dielectric properties of coal samples and thiophenic sulfur compounds**

125 **Fig. 2** shows the variation of dielectric constants of NTC, LGC, benzothiophene and
126 dibenzothiophene with microwave frequency. As indicated in **Fig. 2** (a), the ϵ' value of dibenzothiophene
127 increases with the increased microwave frequency, while that of benzothiophene is on the contrary.
128 Moreover, the ϵ' values of NTC and LGC are higher than benzothiophene and dibenzothiophene. It is
129 considered that coal can store more electric field energy than sulfur compounds in an alternating
130 electromagnetic field [42-45]. **Fig. 2** (b) exhibits that the ϵ'' values of thiophenic sulfur compounds are
131 higher than coal samples, which indicated that sulfur compounds can better convert electric field energy
132 into heat energy [42-45]. When microwave frequency reaches 2 GHz, the induced and oriented
133 polarization occurs in the four samples. Since the microwave frequency is not high, the polarized dipoles
134 have enough time to orient and arrange along the direction of the applied electric field. Most of the input
135 energy of the microwave field is stored in a sample and converted into potential energy. Therefore, when
136 the real part of dielectric constant ϵ' reaches a relatively high value, the imaginary part ϵ'' is usually at a
137 lower level.

138 With the increase of microwave frequency, the change rate of microwave electromagnetic field is
139 accelerated, and the change rate of dipole begins to lag the change rate of microwave field. The
140 interaction between dipoles take place, and the microwave energy is converted into heat energy. At this
141 time, the energy storage decreases, and the energy loss increases [42-45]. There is a peak value of ϵ'' near

142 4 GHz for the four samples, where the microwave frequency reaches the high frequency region above 5
 143 GHz, the change rate of a dipole is completely disconnected from the microwave frequency. The dipole
 144 presents rigidity in the electromagnetic field, and the values of ϵ' and ϵ'' are both in a lower position. Due
 145 to the ϵ'' values of benzothiophene and dibenzothiophene are larger than coal samples, it shows that
 146 thiophenic sulfur compounds produce a dielectric response in the microwave field, and their response
 147 ability to microwave is greater than coal. Therefore, thiophenic sulfur is selectively heated by microwave,
 148 which is conducive to its removal [46].

149



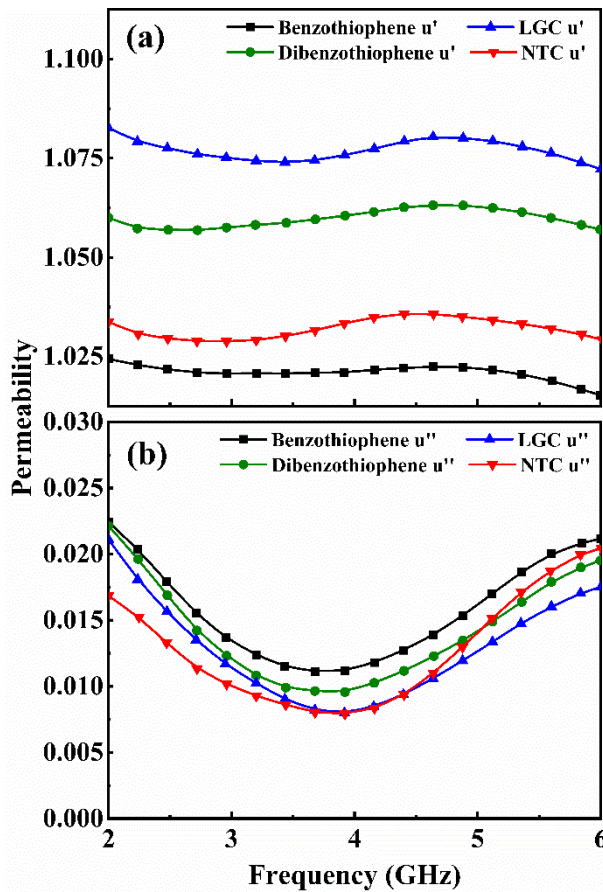
150

151 **Fig. 2. The relation between dielectric constants and microwave frequency; (a) real part and (b) imaginary part.**

152

153 The effects of microwave frequency on μ' and μ'' values of four samples are shown in Fig. 3 (a) and
154 (b), respectively. The results indicate that the μ' value of four samples decrease slightly with the increased
155 microwave frequency. The μ' value of LGC is the largest, while the μ'' values of four samples have no
156 significant difference. Due to the low magnetism properties of the samples, their μ' and μ'' values are at
157 a low level. Therefore, it is considered that both coal and sulfur compounds will not produce a large
158 magnetic response and magnetic loss that is the reason, the influence of magnetic effect on microwave
159 desulfurization of coal can be ignored.

160



161

162 Fig. 3. The relation between permeability and microwave frequency; (a) real part and (b) imaginary part.

163

164 **3.2 Comparison of theoretical microwave absorption power between coal samples and thiophenic**
165 **sulfur compounds**

166 Microwave heating refers to the process that the material absorbs and converts the microwave
167 electric field energy and magnetic field energy into heat energy. In general, the electric field changes
168 along with the space. In special cases, the electric field is regarded as a constant, by using the relation
169 $E \cdot E^* = E^2$, there are Eq. (3) and (4) [47].

170
$$P_{av} = \omega \varepsilon_0 \varepsilon'' \oint (E \cdot E^*) \cdot dV \quad (3)$$

171
$$P_{av} = \omega \varepsilon_0 \varepsilon'' E_{rms}^2 V \quad (4)$$

172 If the material also has a magnetic loss, then above equations is transformed into Eq. (5).

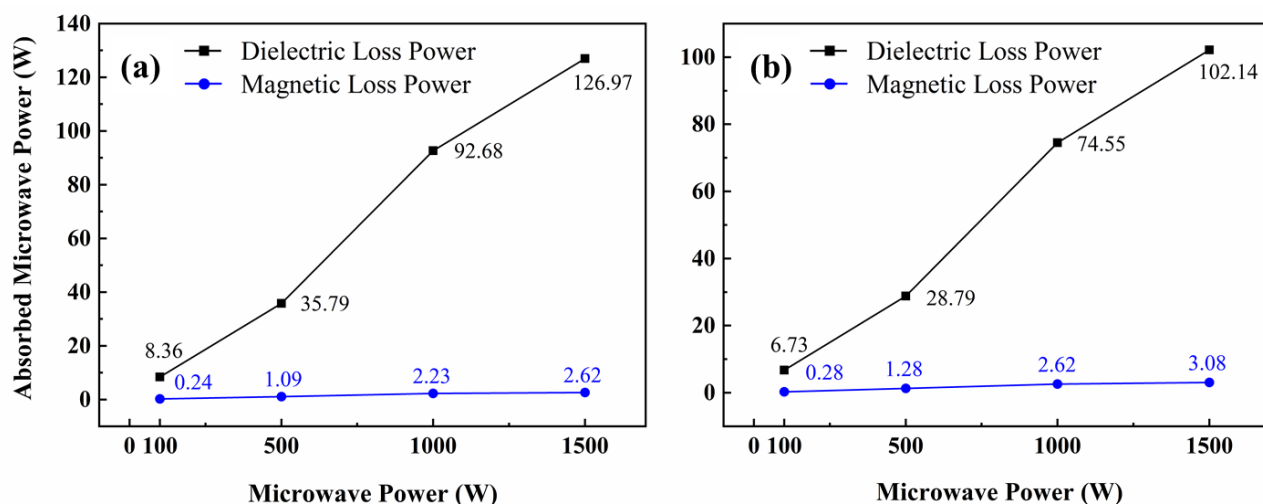
173
$$P_{av} = \omega \varepsilon_0 \varepsilon E_{rms}^2 V + \omega \mu_0 \mu H_{rms}^2 V \quad (5)$$

174 Where P_{av} represents the microwave absorption power in W, E_{rms} represents the effective value of the
175 electric field in V/m, H_{rms} represents the effective value of the magnetic field in A/m. ε_0 and μ_0 are the
176 vacuum dielectric constant and vacuum permeability of sample, respectively, which are regarded as
177 constants under certain conditions. V represents the volume of the sample in m^3 .

178 In order to explain the dielectric response mechanism of coal desulfurization by microwave, the
179 theoretical microwave absorption power of samples is estimated by the measuring dielectric constant and
180 permeability value as in Eq. (5). The equivalent electromagnetic field is set based on the results of
181 previous studies (15254.42 V/M and 2.33 A/M) [36], and the microwave input power is set at 1000 W
182 [35].

183 **Fig. 4** shows the heat generated by the dielectric loss (equivalent to the heat absorbed from the
 184 microwave electric field) and magnetic loss of coal samples as a function of microwave frequency. In
 185 2.45 GHz region, the dielectric loss of coal samples occupy the dominant position and the generated heat
 186 is much greater than magnetic loss [42]. For example, the dielectric loss of NTC is about 92.68 W at
 187 1000 W microwave power, while the magnetic loss is only 2.23 W. Similarly, the dielectric loss LGC is
 188 about 74.55 W at the frequency of 1000 W, while the magnetic loss is only 2.62 W.

189



190

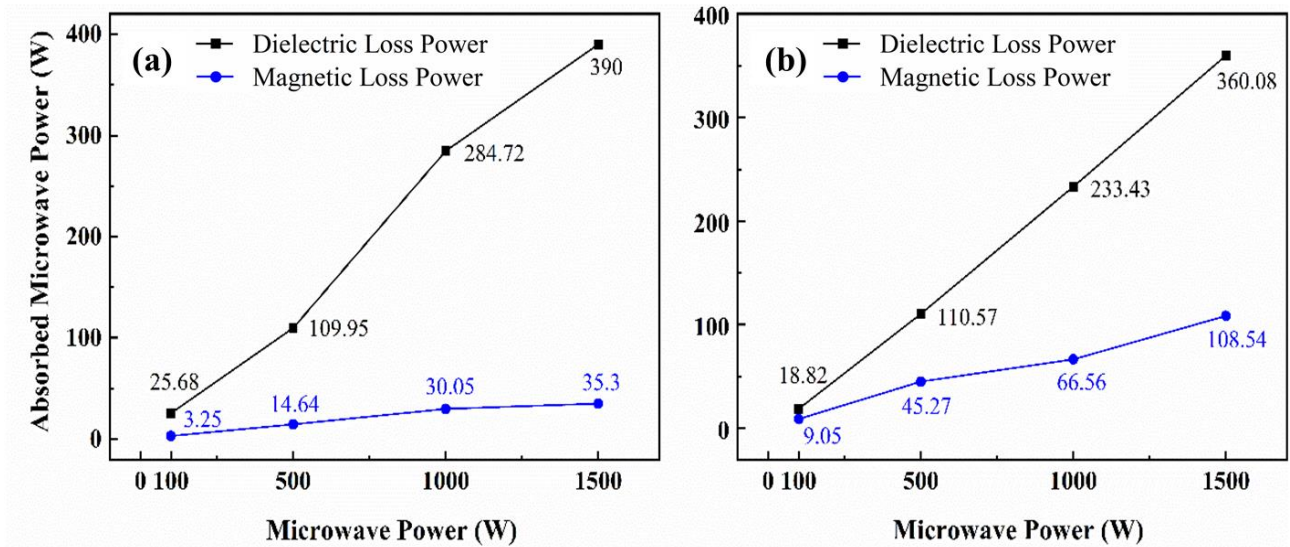
191 **Fig. 4. Theoretical microwave absorption power at 2.45GHz; (a) NTC and (b) LGC.**

192

193 The dielectric loss power of benzothiophene is higher than coal samples as shown in **Fig. 5**. For
 194 example, under 1000 W microwave power, the dielectric loss power of LGC is about 74.55 W, while
 195 benzothiophene is 284.72 W. Moreover, the heating power generated by the magnetic loss of
 196 benzothiophene is also relatively larger. The magnetic loss of LGC is 2.62 W while benzothiophene is
 197 30.05 W at 1000 W. The dielectric loss of benzothiophene is still dominant [48]. Dibenzothiophene also

198 shows the same characteristics as benzothiophene, under microwave irradiation, its heat absorption is
 199 greater than coal sample; its own dielectric loss is much higher than the magnetic loss. At 1000 W
 200 microwave power, the dielectric loss power of dibenzothiophene is 233.43 W, and the magnetic loss
 201 power is 66.56 W. Due to the small value of the equivalent magnetic field, their magnetic loss is also
 202 very low. Due to the equivalent magnetic field values of coal samples and thiophenic sulfur compounds
 203 are very small, their magnetic losses are also very low. Therefore, the dielectric response is the main
 204 effect of microwave effect and the research on the microwave effect should focus on the influence of the
 205 microwave electric field [23, 33].

206



207

208 **Fig. 5. Theoretical microwave absorption power at 2.45GHz; (a) benzothiophene and (b) dibenzothiophene.**

209

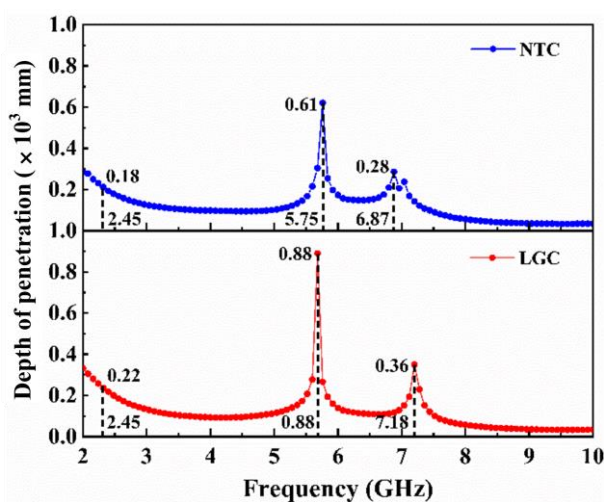
210 According to the measured dielectric constants, the penetration depth D_p of the electromagnetic
 211 wave to the sample is calculated as follows Eq. (6) [49].

212
$$D_p = \lambda'_0 / [2\pi(2\epsilon')^{1/2}] * [(1 + (\epsilon''/\epsilon')^2)^{1/2} - 1]^{-1/2} \quad (6)$$

213 where λ'_0 represents the wavelength of the incident wave in mm.

214 The calculated penetration depth is shown in Fig. 6. NTC has large microwave penetration depth at
215 5.75, 6.87 and 7.06 GHz, which are 610, 280 and 230 mm respectively; LGC has large microwave
216 penetration depth at 5.67 and 7.18 GHz, which are 880 and 360 mm respectively. However, at 2.45GHz
217 (Universal microwave frequency), the penetration depth of NTC and LGC can reach 180 mm and 220
218 mm respectively, which is larger than the general particle size of coal samples. The results indicate that
219 the effect of microwave on desulfurization of coal is not only limited to the surface of coal but also has
220 the same effect on sulfur groups in coal when the microwave frequency is appropriate [49, 50].

221



222

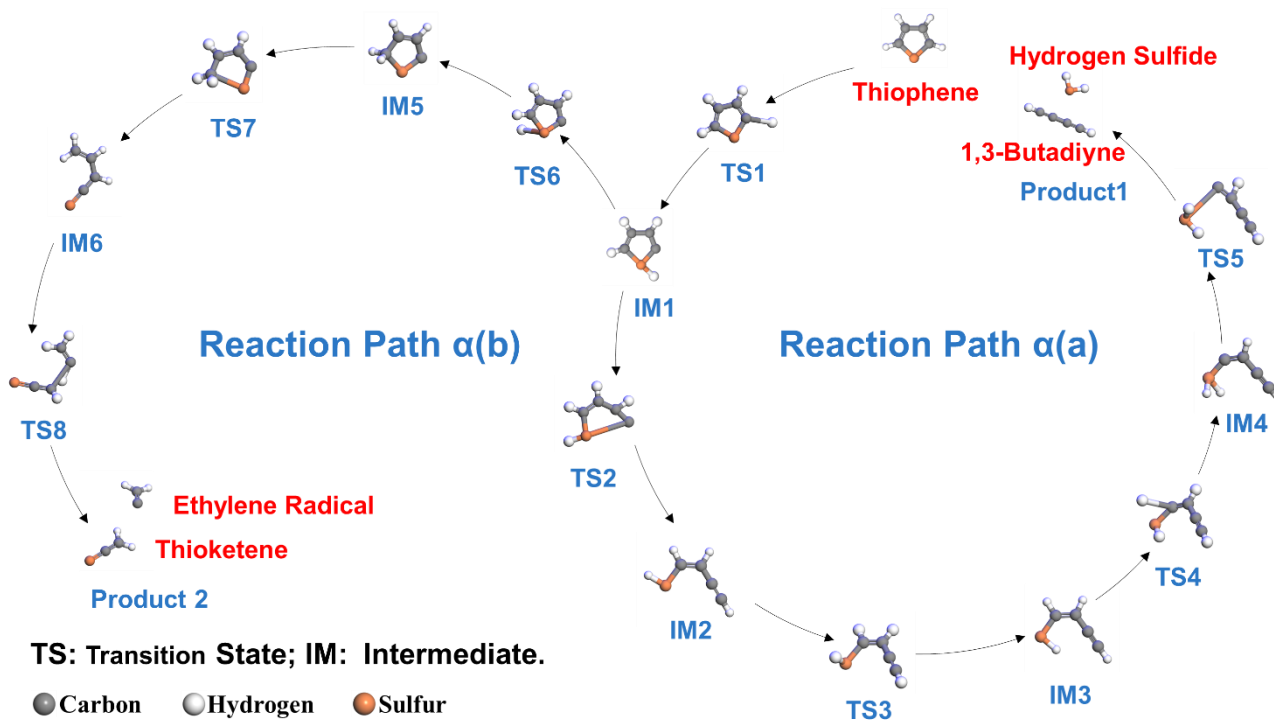
223 Fig. 6. Microwave penetration depth of NTC and LGC as a function of microwave frequency.

224

225 3.3 Thiophenic sulfur migration pathway

226 The transfers of α -H to S atom, referring to α (a) and α (b) are shown in Fig. 7. For the α (a) process,
227 the α -H on thiophene first migrates to the adjacent S atom to form IM1, and then the thiophene ring

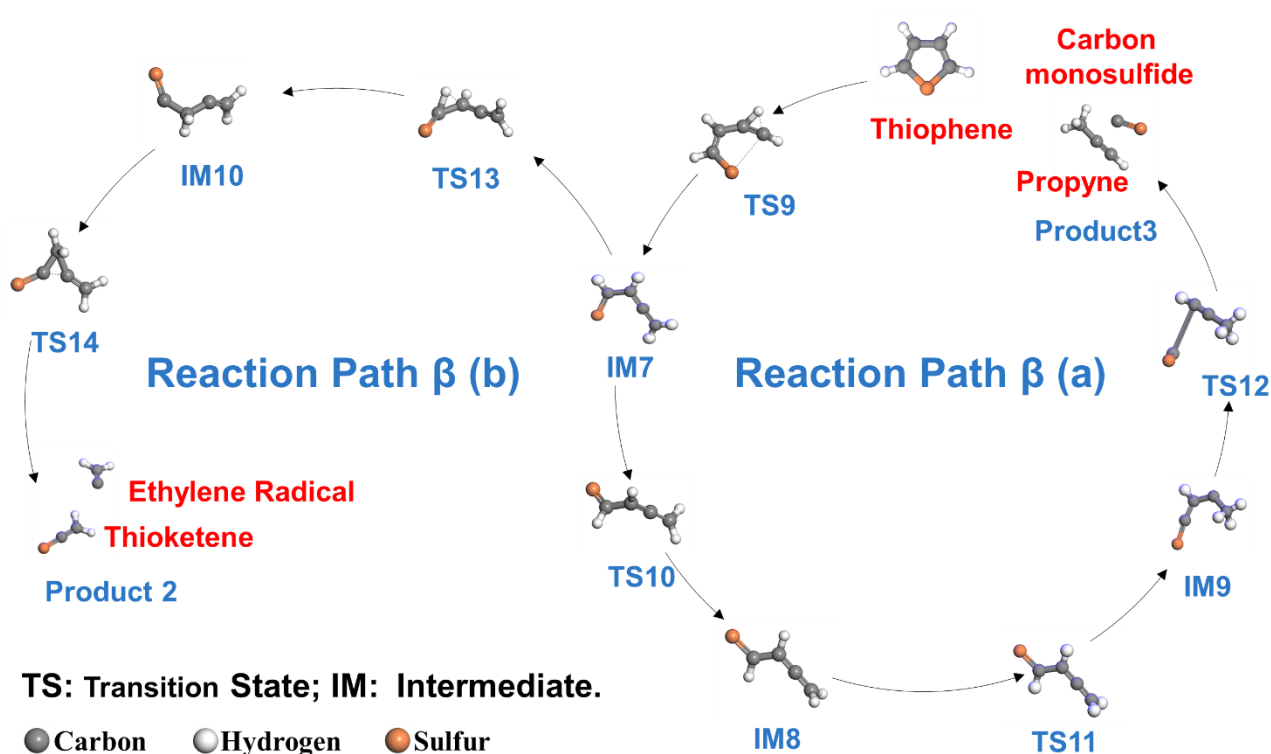
228 breaks twice to form hydrogen sulfide and 1,3-butanediyne (Product 1). In addition, H on the S atom of
 229 IM1 may continue to migrate to form ethylene radical and thioketene (Product 2), named as $\alpha(b)$ process.
 230



231
 232 **Fig. 7. α desulfurization reaction path; (a) generate H₂S and 1,3-butadiyne and (b) generate ethylene radical**
 233 **and thioketene.**

234 **Fig. 8** reveals the migration of β -H to α -C, referred to as $\beta(a)$ and $\beta(b)$ respectively. $\beta(a)$ is that the
 235 β -H on thiophene first migrates to the adjacent α -C, at the same time, the C-S bond breaks to form IM7.
 236 In this step, the thiophene ring finally forms carbon monosulfide and propyne (product 3). Moreover, the
 237 H on another α -C of IM7 continues to migrate to form ethylene radical and thioketene (product 2), which
 238 is named $\beta(b)$ process and its final product is the same as $\alpha(b)$ process.

239



240

241 **Fig. 8. β desulfurization reaction path; (a) generate carbon monosulfide and propyne and (b) generate ethylene**
 242 **radical and thioketene.**

243

244 3.4 Comparison of E_b of thiophenic sulfur removal process before and after adding microwave field

245

E_b represents the zero-point energy difference between the activated complex and reactant. The

246

larger the E_b is, the more difficult the reaction. As presented in **Fig. 9**, the external electric field hinders

247

the $\alpha(a)$ process for Rea to IM2, and its E_b increases from 214.23 to 238.58 $\text{kJ}\cdot\text{mol}^{-1}$. However, the

248

process from IM3 to IM4 becomes easier under the external electric field and its E_b decreases from

249

477.73 to 253.76 $\text{kJ}\cdot\text{mol}^{-1}$. For $\alpha(b)$ process, the E_b from Rea to IM5 is increased by the applied electric

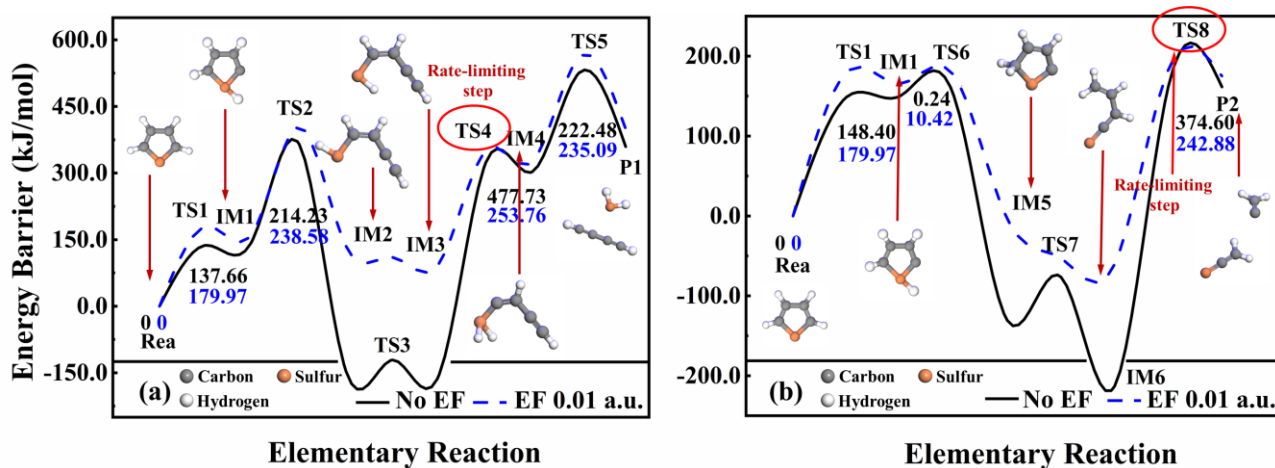
250

field, but the reaction process from IM5 to IM6 becomes an incompetent barrier reaction. The E_b of the

251

process from IM6 to P2 is reduced from 374.60 to 242.88 $\text{kJ}\cdot\text{mol}^{-1}$, which is the most difficult step in the

252 whole reaction process. Therefore, it is considered that the applied electric field can effectively reduce
 253 reaction difficulty. By comparing the maximum E_b of the above two reaction paths, it can be concluded
 254 that compared with $\alpha(a)$, $\alpha(b)$ is more suitable for H atom migration in the process of removing thiophenic
 255 sulfur from coal microwave [43].

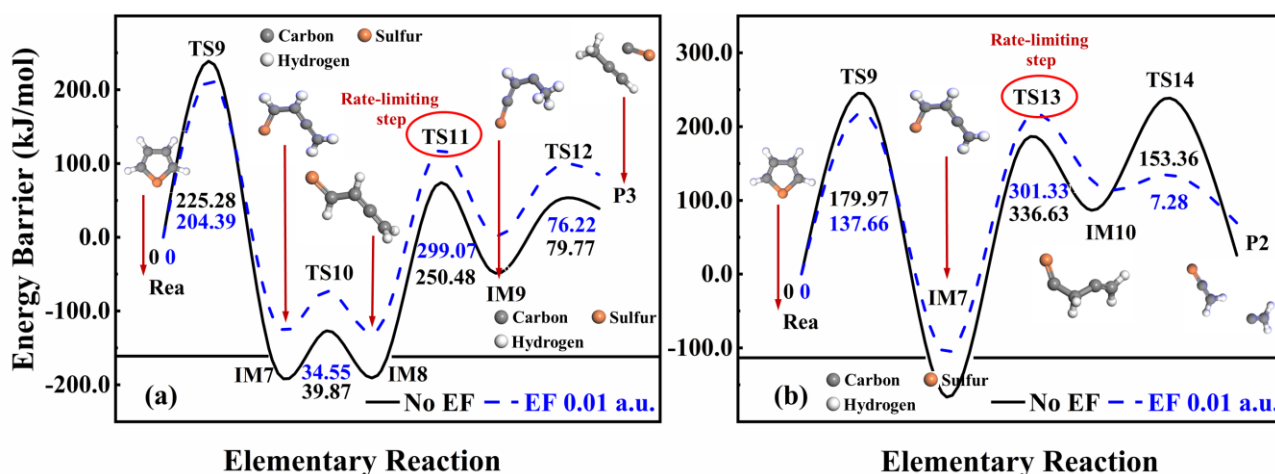


257 **Elementary Reaction** **Elementary Reaction**
 258 **Fig. 9. The energy barrier E_b of thiophenic sulfur removal by pathway α ; (a) $\alpha(a)$ pathway and (b) $\alpha(b)$**
 259 **pathway.**

260
 261 **Fig. 10** shows the change of E_b of thiophenic sulfur removal by pathway β . For the $\beta(a)$ reaction
 262 path, the external electric field promotes the processes of Rea to IM7, IM7 to IM8 and IM9 to P3. The
 263 E_b decreases from 225.28 to 204.39 $\text{kJ}\cdot\text{mol}^{-1}$, and 79.77 to 76.22 $\text{kJ}\cdot\text{mol}^{-1}$, respectively. However, the
 264 reaction from IM8 to IM9 is inhibited by the applied electric field, which is the rate-limiting step of the
 265 $\beta(a)$ path. The E_b of IM8 to IM9 is increased from 250.48 to 299.07 $\text{kJ}\cdot\text{mol}^{-1}$. Therefore, it can be
 266 considered that microwave can inhibit the removal of thiophenic sulfur for this route. For the $\beta(b)$
 267 reaction path, the external electric field promotes the progress of all elementary reactions, especially in

268 the rate-limiting step IM7 to IM10, where the E_b decreases from 336.63 to 301.33 kJ·mol⁻¹. Comparing
 269 the above results, it is found that although microwave promotes the occurrence of the $\beta(b)$ pathway, the
 270 E_b of rate-limiting step (301.33) is still higher than that of $\beta(a)$ path (299.07). That is, the β -H atoms tend
 271 to migrate according to $\beta(a)$, and this trend is inhibited under the microwave irradiation. Finally,
 272 combined with Fig. 9 and 10, it can be concluded from the E_b of rate-limiting step of different reaction
 273 path that under microwave irradiation, the optimal removal path of thiophenic sulfur will change from
 274 $\beta(a)$ to $\alpha(b)$, and be catalyzed by microwave.

275



276

277 **Fig. 10. The energy barrier E_b of thiophenic sulfur removal by pathway β ; (a) $\beta(a)$ pathway and (b) $\beta(b)$**
 278 **pathway.**

279

280

281 **3.5 Comparison of E_a and $\ln k$ of thiophenic sulfur removal process before and after adding microwave field**

282

E_a and $\ln k$ represent the difficulty and speed of the chemical reaction respectively, which can be

283 calculated by Eq. (7) ~ (8). According to the transition state theory of Eyring chemical reaction, the molar
 284 statistical enthalpy ($\Delta_r H_m$) and entropy ($\Delta_r S_m$) of each elementary reaction in thiophenic sulfur
 285 migration path can be obtained. The calculation formula and obtained results are shown in Eq. (9) ~ (10)
 286 and supplementary Table S-1, respectively.

$$287 \quad E_a = \Delta_r H_m + nRT \quad (7)$$

$$288 \quad \ln k = \ln \left(\frac{KT}{h} e^{-\frac{E_a}{RT}} \cdot e^{\frac{\Delta_r S_m}{RT}} \right) \quad (8)$$

289 where n , R , T , K and h represent the molar mass of substance, gas constant (8.314 J/mol·K), reaction
 290 temperature (K), Boltzmann constant (1.38×10^{-23} J/K) and Planck constant (6.63×10^{-34} J·s), respectively.

$$291 \quad \Delta_r H_m = E_{total}(TS) + H_m^0(TS) - E_{total}(R) + H_m^0(R) \quad (9)$$

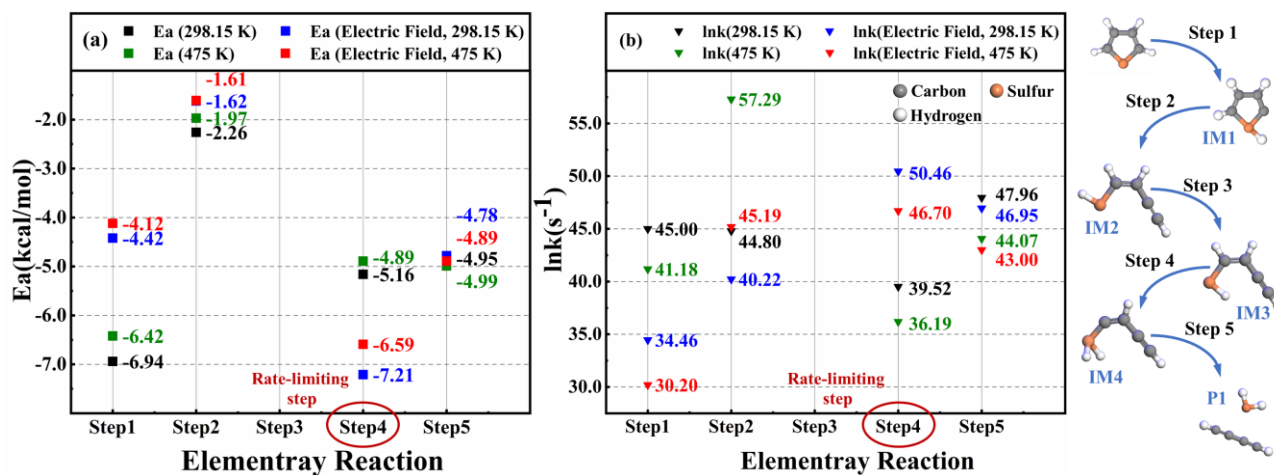
$$292 \quad \Delta_r S_m = S_m^0(TS) - S_m^0(R) \quad (10)$$

293 Where E_{total} , TS and R represent the total energies, the transitions and the reactants, respectively.

294 **Fig. 11** presents the process of $\alpha(a)$ reaction of thiophene to produce hydrogen sulfide and 1,3-
 295 butadiyne. It can be seen from the figure that except step 4, increasing temperature or applying electric
 296 field increases E_a and decreases $\ln k$ in each step of the reaction, and the effect of electric field is more
 297 significant. Step 4 is the hydrogen transfer reaction. And this step is the rate-limiting step in $\alpha(a)$ reaction
 298 process, which needs to cross the highest E_b in **Fig. 9**. The whole reaction speed is determined by the
 299 speed of this step. Under the condition of no electric field, the $\ln k$ in step 4 is 39.52 and 36.19 at 298.15
 300 and 475 K respectively, which is the smallest in the whole reaction. After applying electric field, the $\ln k$
 301 of this step increases to 50.46 and 46.70 at 298.15 K and 475 K respectively. Therefore, combined with
 302 **Fig. 9 (a)**, it can be considered that the presence of microwave field not only reduces the difficulty of

303 hydrogen migration along $\alpha(a)$, but also speeds up the reaction, thus catalyzing removal of thiophenic
 304 sulfur [40-44, 48].

305



306

307 **Fig. 11.** E_a and $\ln k$ of elementary reactions in $\alpha(a)$ reaction pathway; (a) E_a and (b) $\ln k$.

308

309 **Fig. 12** reflects E_a and $\ln k$ of elementary reactions in $\alpha(b)$ pathway, and the change of temperature
 310 has little effect on E_a and $\ln k$. After the addition of electric field, the E_a of Step 1 and step 2 increases,
 311 while that of step 3 and step 4 decreases, indicating that the electric field inhibits the progress of the first
 312 two reactions and promotes the latter two reactions. This is consistent with the results of previous studies
 313 [23, 40]. Reviewing **Fig. 9 (b)**, step 3 and 4 are C–S and C–C bond-breaking reaction respectively, and
 314 step 4 is the rate limiting step of $\alpha(b)$ pathway. Therefore, it is believed that the microwave field promotes
 315 the C–C bond breaking, thus catalyzing the removal of thiophenic sulfur along $\alpha(b)$ pathway.

316

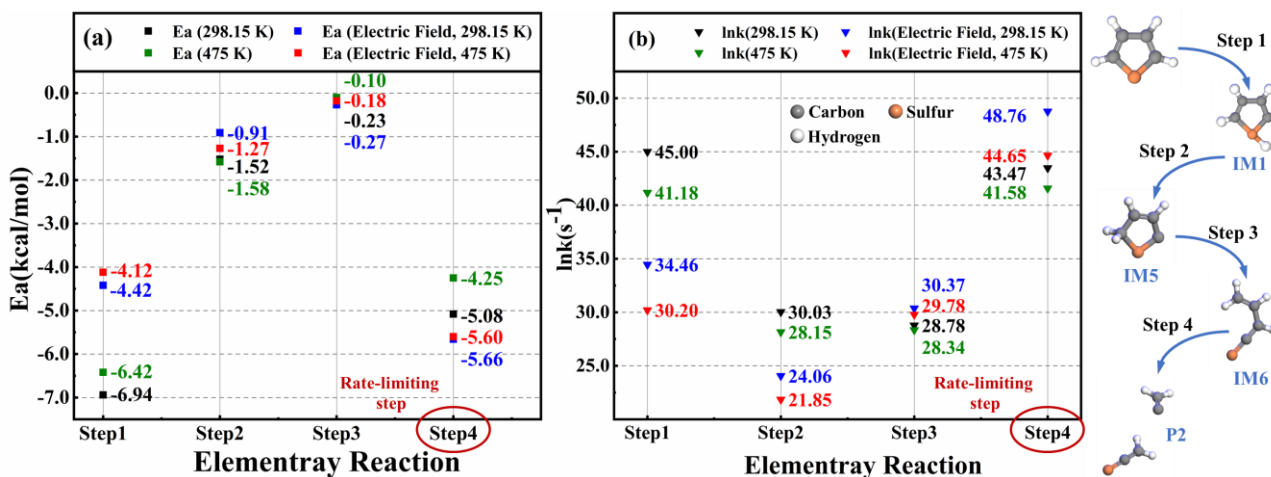


Fig. 12. E_a and $\ln k$ of elementary reactions in $\alpha(b)$ reaction pathway; (a) E_a and (b) $\ln k$.

317

318

319

320 E_a and $\ln k$ of elementary reactions in $\beta(a)$ reaction pathway to produce carbon monosulfide and

321 propyne are illustrated in Fig. 13. Elevated temperature has little effect on E_a and $\ln k$ of the reaction, but

322 the applied electric field obviously improves $\ln k$ of step 1 and lowers that of step 2, 3 and 4. In

323 combination with Fig. 10 (a), step 3 representing the hydrogen migration between carbon atoms is the

324 rate limiting step of $\beta(a)$ pathway. It is assumed that the external microwave not only improves E_b of

325 hydrogen migration along $\beta(a)$, but also reduces its reaction rate, thus inhibiting removal of thiophenic

326 sulfur.

327

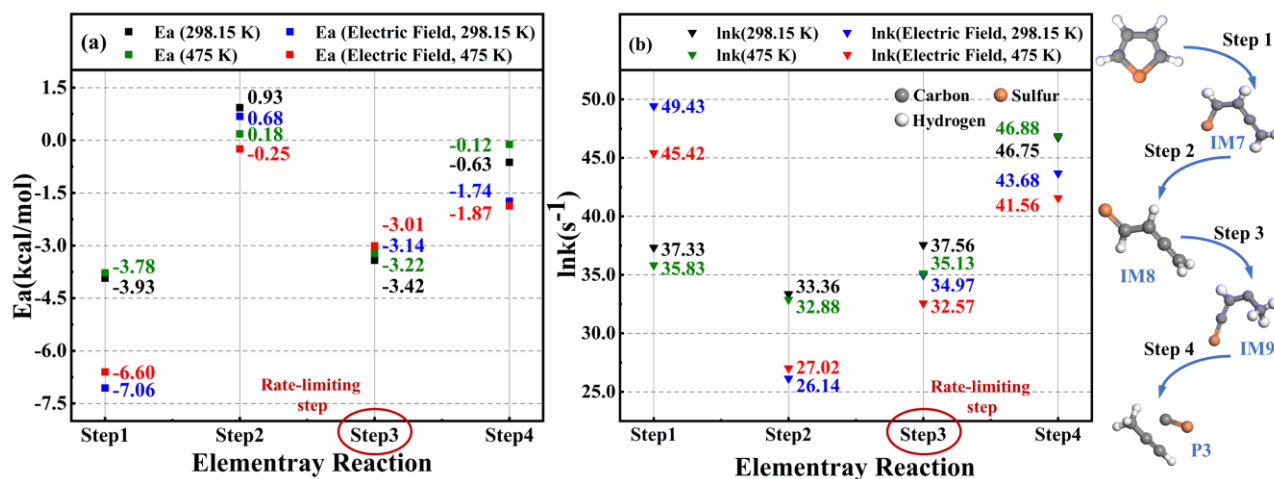


Fig. 13. E_a and $\ln k$ of elementary reactions in β (a) reaction pathway; (a) E_a and (b) $\ln k$.

328

329

330

331

332

333

334

335

336

337

338

Fig. 14 shows the E_a and $\ln k$ of elementary reactions in β (b) reaction pathway that represents thiophene generates ethylene radicals and thioketene. E_a of each step of the pathway decreases after the addition of electric field, which indicates that the applied microwave field promotes the reaction rate of each step. Combining with Fig. 10 (b), it shows that step 2 of hydrogen migration between carbon atoms is the rate limiting step of β (b) pathway. Therefore, it is considered that microwave can improve the removal of thiophenic sulfur from coal along β (b) pathway by catalytic cracking of C–H bonds [40-44, 48].

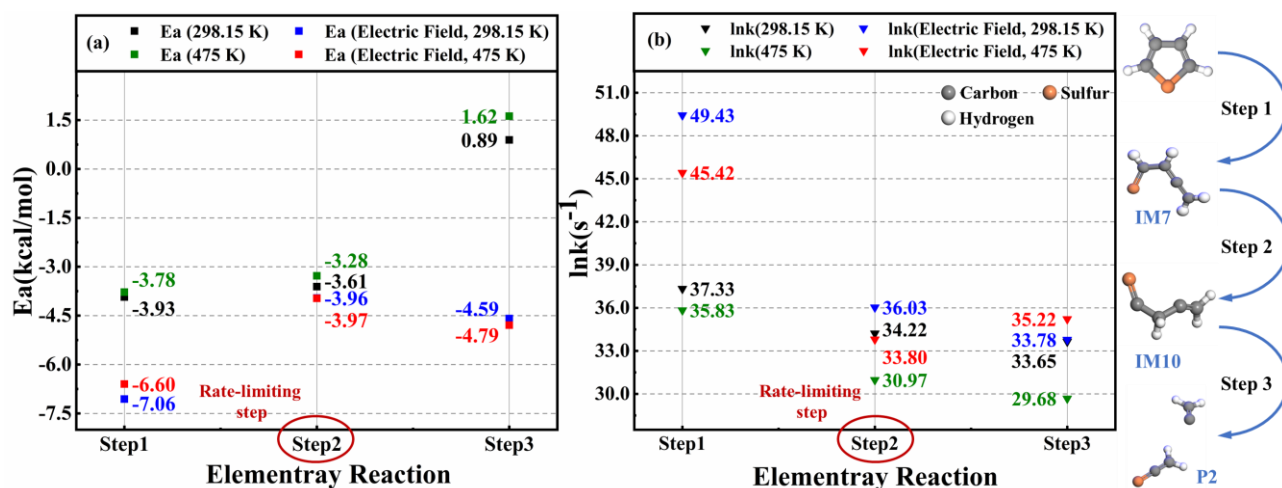


Fig. 14. E_a and $\ln k$ of elementary reactions in $\beta(b)$ reaction pathway; (a) E_a and (b) $\ln k$.

Based above result, After the application of microwave field, the minimum E_b path of thiophene sulfur remove from coal is transferred from $\beta(a)$ to $\alpha(b)$, and the E_a of rate-limiting step for $\beta(a)$ is increased and the $\ln k$ is decreased, while the $\alpha(b)$ is on the contrary. On the whole, the E_a and $\ln k$ of $\alpha(b)$ with microwave is better than that of $\beta(a)$ without microwave.

Table 2 Thermodynamics and kinetics parameters of rate-limiting step at 298.15 K

Reaction path	Thermodynamics and kinetics parameters of rate-limiting step at 298.15 K					
	E_b	E_b -EF	E_a	E_a -EF	$\ln k$	$\ln k$ -EF
$\alpha(a)$	477.73	253.76	-5.16	-7.21	39.52	50.46
$\alpha(b)$	374.60	242.88	-5.08	-5.66	43.47	48.76
$\beta(a)$	250.48	299.07	-3.42	-3.14	37.56	34.97
$\beta(b)$	336.63	310.33	-3.61	-3.96	34.22	36.02

EF: Electric field

349 **4 Conclusions**

350 By measuring the dielectric properties, it is found that the imaginary part of dielectric constants ϵ''
351 of benzothiophene and dibenzothiophene is higher than coal samples, which means that thiophenic sulfur
352 compounds in coal can generate more heat with microwave irradiation. So, thiophenic sulfur can be
353 selectively heated by microwave. In addition, due to the weak magnetic properties of coal samples and
354 thiophenic sulfur, the heating value from magnetic loss is far lower than the dielectric loss, so the
355 microwave field is simplified to an electric field in the simulation. Linear Synchronous Transit/Quadratic
356 Synchronous Transit transition state search shows that under microwave irradiation, the cleavage of C–H
357 or C–C bond in paths $\alpha(a)$, $\alpha(b)$ and $\beta(b)$ was catalyzed and the cleavage of C–H bond in path $\beta(a)$ was
358 inhibited, resulting in the change of the optimal removal path of thiophenic sulfur from $\beta(a)$ to $\alpha(b)$ and
359 sulfur-containing products changed from carbon monosulfide (CS) to thioketene (C_2H_2S). Overall, the
360 calculated thermodynamic and kinetic parameters of rate limiting steps of each reaction pathway
361 indicated that that the applied microwave can catalyze the removal of thiophenic sulfur by reducing E_b
362 and E_a and increasing $\ln k$.

363 **Acknowledgements**

364 The work is supported by the National Natural Science Foundation of China (Project No. 51774061
365 & 52074055) and Chongqing Talent program (Project No. CQYC201905039). The authors also thank
366 Mr. Yang Zhang (Ingle Testing Technology Services (Shanghai) Co., Ltd) for the support of dielectric
367 measurement.

368 **Conflict of interest statement**

369 On behalf of all authors, the corresponding author states that there is no conflict of interest.

370 **References**

- 371 [1] NBOS. China, The 2019 National economic and social development statistics bulletin of the people's
372 republic of China (PRC), NBS, Beijing, 2019, <https://doi.org/10.38309/n.cnki.nzgxx.2020.000341>.
- 373 [2] Tang Y, He X, Chen A, Li W, Deng X, Wei Q, Occurrence and sedimentary control of sulfur in coals
374 of China, *J. China Coal Soc* 2015;40:1977-1988.
- 375 [3] Liu J, Reflection on low-carbon development of coal energy in China, *Journal of China University
376 of Mining and Technology (Social Science edition)*, 2011, 13, 5-12.
- 377 [4] Lotfian S, Ahmed H, Samuelsson C. Alternative reducing agents in metallurgical processes:
378 devolatilization of shredder residue materials. *J SUST METALL* 2017;3(2):311-21.
379 <https://doi.org/10.1007/s40831-016-0094-0>
- 380 [5] Nomura S. Use of waste plastics in coke oven: a review. *J SUST METALL* 2015;1(1):85-93.
381 <https://doi.org/10.1007/s40831-014-0001-5>
- 382 [6] Delley B. From molecules to solids with the DMol(3) approach. *J Chem Phys* 2000;113(18):7756-
383 64. <https://doi.org/10.1063/1.1316015>.
- 384 [7] Yang N, Guo H, Liu F, Zhang H, Hu Y, Hu R. Effects of atmospheres on sulfur release and its
385 transformation behavior during coal thermolysis. *Fuel* 2018;215:446-53.
386 <https://doi.org/10.1016/j.fuel.2017.11.099>.

- 387 [8] Kawashima H. Changes in sulfur functionality during solvent extraction of coal in Hyper-coal
388 production. *Fuel Process Technol* 2019;188:105-9. <https://doi.org/10.1016/j.fuproc.2019.02.011>.
- 389 [9] Chen H, Huo Q, Wang Y, Han L, Lei Z, Wang J, et al. Upcycling coal liquefaction residue into sulfur-
390 rich activated carbon for efficient Hg⁰ removal from coal-fired flue gas. *Fuel Process Technol*
391 2020;206. <https://doi.org/10.1016/j.fuproc.2020.106467>.
- 392 [10] Meng X, Li L, Li K, Zhou P, Zhang H, Jia J, et al. Desulfurization of fuels with sodium borohydride
393 under the catalysis of nickel salt in polyethylene glycol. *J Clean Prod* 2018;176:391-8.
394 <https://doi.org/10.1016/j.jclepro.2017.12.152>.
- 395 [11] Tang L, Chen S, Wang S, Tao X, He H, Zheng L, et al. Heterocyclic sulfur removal of coal based on
396 potassium tert-butoxide and hydrosilane system. *Fuel Process Technol* 2018;177:194-9.
397 <https://doi.org/10.1016/j.fuproc.2018.04.031>.
- 398 [12] Zhang B, Zhu G, Lv B, Dong L, Yan G, Zhu X, et al. A novel high-sulfur fine coal clean
399 desulfurization pretreatment : Microwave magnetic separation, high-gradient effect and magnetic
400 strengthen. *J Clean Prod* 2018;202:697-709. <https://doi.org/doi.org/10.1016/j.jclepro.2018.08.088>.
- 401 [13] Tao X, Xu N, Xie M, Tang L. Progress of the technique of coal microwave desulfurization. *Int J*
402 *Coal Sci Technol* 2014;1(1):113-28. <https://doi.org/10.1007/s40789-014-0006-5>.
- 403 [14] Pecina ET, Camacho LF, Herrera CA, Martinez D. Effect of complexing agents in the
404 desulphurization of coal by H₂SO₄ and H₂O₂ leaching. *Miner Eng* 2012;29:121-3.
405 <https://doi.org/10.1016/j.mineng.2011.10.011>.

- 406 [15]Blaesing M, Melchior T, Mueller M. Influence of temperature on the release of inorganic species
407 during high temperature gasification of Rhenish lignite. *Fuel Process Technol* 2011;92(3):511-6.
408 <https://doi.org/10.1016/j.fuproc.2010.11.005>.
- 409 [16]Jorjani E, Rezai B, Vossoughi M, Osanloo M, Abdollahi M. Oxidation pretreatment for enhancing
410 desulfurization of coal with sodium butoxide. *Miner Eng* 2004;17(4):545-52.
411 <https://doi.org/10.1016/j.mineng.2003.12.007>.
- 412 [17]Jorjani E, Chelgani SC, Mesroghli S. Application of artificial neural networks to predict chemical
413 desulfurization of Tabas coal. *Fuel* 2008;87(12):2727-34. <https://doi.org/10.1016/j.fuel.2008.01.029>.
- 414 [18]Wijaya N, Choo TK, Zhang L. Generation of ultra-clean coal from Victorian brown coal - Sequential
415 and single leaching at room temperature to elucidate the elution of individual inorganic elements.
416 *Fuel Process Technol* 2011;92(11):2127-37. <https://doi.org/10.1016/j.fuproc.2011.05.022>.
- 417 [19]Zhang B, Ma Z, Zhu G, Yan G, Zhou C. Clean coal desulfurization pretreatment: microwave
418 magnetic separation, Response Surface, and Pyrite Magnetic Strengthen. *Energy Fuels*
419 2018;32(2):1498-505. <https://doi.org/10.1021/acs.energyfuels.7b03561>.
- 420 [20]Wiser WH. Conversion of bituminous coal to liquids and gases: chemistry and representative
421 processes. In: Petrakis L, Fraissard JP, editors. Petrakis L, Fraissard JP Springer Netherlands
422 Dordrecht; 1984, p. 325-50. https://doi.org/10.1007/978-94-009-6378-8_12.
- 423 [21]Zhang L, Wang Y, Li X, Wang S. Region-of-interest extraction based on spectrum saliency analysis
424 and coherence-enhancing diffusion model in remote sensing images. *Neurocomputing*

- 425 2016;207:630-44. <https://doi.org/10.1016/j.neucom.2016.05.045>.
- 426 [22] Tang L, Long K, Chen S, Gui D, He C, Li J, et al. Removal of thiophene sulfur model compound
427 for coal by microwave with peroxyacetic acid. *Fuel* 2020;272:117748.
428 <https://doi.org/10.1016/j.fuel.2020.117748>.
- 429 [23] Jorjani E, Chelgani SC, Mesroghli S. Prediction of microbial desulfurization of coal using artificial
430 neural networks. *Miner Eng* 2007;20(14):1285-92. <https://doi.org/10.1016/j.mineng.2007.07.003>.
- 431 [24] Qin ZH, Zhang HF, Dai DJ, Zhao CC, Zhang LF. Study on occurrence of sulfur in different group
432 components of Xinyu clean coking coal. *Journal of Fuel Chemistry and Technology*
433 2014;42(11):1286-94.
- 434 [25] Tang L, Chen S, Wang S, Tao X, He H, Fan H. Exploration of the combined action mechanism of
435 desulfurization and ash removal in the process of coal desulfurization by microwave with
436 peroxyacetic acid. *Energy Fuels* 2017;31(12):13248-58.
437 <https://doi.org/10.1021/acs.energyfuels.7b02112>.
- 438 [26] Yao Q, Sun M, Gao J, Wang R, Zhang Y, Xu L, et al. Organic sulfur compositions and distributions
439 of tars from the pyrolysis of solvent pretreatment vitrinite of high sulfur coal. *J Anal Appl Pyrolysis*
440 2019;139:291-300. <https://doi.org/10.1016/j.jaap.2019.03.002>.
- 441 [27] Saikia BK, Khound K, Baruah BP. Extractive desulfurization and deashing of high sulfur coals by
442 oxidation with ionic liquids. *Energy Convers Manage* 2014;81:298-305.
443 <https://doi.org/10.1016/j.enconman.2014.02.043>.

- 444 [28]Mursito AT, Hirajima T, Sasaki K. Alkaline hydrothermal de-ashing and desulfurization of low
445 quality coal and its application to hydrogen-rich gas generation. *Energy Convers Manage*
446 2011;52(1):762-9. <https://doi.org/10.1016/j.enconman.2010.08.001>.
- 447 [29]Bichot A, Lerosty M, Radoiu M, Méchin V, Bernet N, Delgenès J-P, et al. Decoupling thermal and
448 non-thermal effects of the microwaves for lignocellulosic biomass pretreatment. *Energy Convers*
449 *Manage* 2020;203. <https://doi.org/10.1016/j.enconman.2019.112220>.
- 450 [30]Mong GR, Chong CT, Ng JH, Chong WWF, Lam SS, Ong HC, et al. Microwave pyrolysis for
451 valorization of horse manure biowaste. *Energy Convers Manage* 2020;220.
452 <https://doi.org/10.1016/j.enconman.2020.113074>.
- 453 [31]Wu Q, Wang Y, Peng Y, Ke L, Yang Q, Jiang L, et al. Microwave-assisted pyrolysis of waste cooking
454 oil for hydrocarbon bio-oil over metal oxides and HZSM-5 catalysts. *Energy Convers Manage*
455 2020;220. <https://doi.org/10.1016/j.enconman.2020.113124>.
- 456 [32]Cai SS, Zhang SF, Wei Y, Sher F, Wen LY, Xu J, et al. A novel method for removing organic sulfur
457 from high-sulfur coal: Migration of organic sulfur during microwave treatment with NaOH-H₂O₂.
458 *Fuel* 2021;289:119800. <https://doi.org/10.1016/j.fuel.2020.119800>.
- 459 [33]Liu J, Wang Z, Qiao Z, Chen W, Zheng L, Zhou J. Evaluation on the microwave-assisted chemical
460 desulfurization for organic sulfur removal. *J Clean Prod* 2020;267:121878.
461 <https://doi.org/10.1016/j.jclepro.2020.121878>.
- 462 [34]Wu Y, Zhang SF, Cai SS, Xiao X, Yin C, Xu J, et al. Transformation of organic sulfur and its

- 463 functional groups in nantong and laigang coal under microwave irradiation. *J Comput Chem*
464 2019;40(31):2749-60. <https://doi.org/10.1002/jcc.26051>.
- 465 [35] Tao X, Tang L, Xie M, He H, Xu N, Feng L, et al. Dielectric properties analysis of sulfur-containing
466 models in coal and energy evaluation of their sulfur-containing bond dissociation in microwave field.
467 *Fuel* 2016;181:1027-33. <https://doi.org/10.1016/j.fuel.2016.05.005>.
- 468 [36] Nicolson AM, Ross GF. Measurement of the intrinsic properties of materials by time-domain
469 techniques. *IEEE Trans Instrum Meas* 1970;IM-19(4):377-82.
470 <https://doi.org/10.1109/TIM.1970.4313932>.
- 471 [37] Song X, Parish CA. Pyrolysis mechanisms of thiophene and methylthiophene in asphaltenes. *J Phys*
472 *Chem A* 2011;115(13):2882-91. <https://doi.org/10.1021/jp1118458>.
- 473 [38] Ling LX, Zhang RG, Wang BJ, Xie KC. DFT study on the sulfur migration during benzenethiol
474 pyrolysis in coal. *J M Struc-Theochem* 2010;952(1-3):31-5.
475 <https://doi.org/10.1016/j.theochem.2010.04.001>.
- 476 [39] Ling LX, Zhang RG, Wang BJ, Xie KC. Density functional theory study on the pyrolysis mechanism
477 of thiophene in coal. *J M Struc-Theochem* 2009;905(1-3):8-12.
478 <https://doi.org/10.1016/j.theochem.2009.02.040>.
- 479 [40] Zhang F, Guo H, Liu Y, Liu F, Hu R. Theoretical study on desulfurization mechanisms of a coal-
480 based model compound 2-methylthiophene during pyrolysis under inert and oxidative atmospheres.
481 *Fuel* 2019;257:116028. <https://doi.org/10.1016/j.fuel.2019.116028>.

- 482 [41] Fan W, Jia C, Hu W, Yang C, Liu L, Zhang X, et al. Dielectric properties of coals in the low-terahertz
483 frequency region. *Fuel* 2015;162:294-304. <https://doi.org/10.1016/j.fuel.2015.09.027>.
- 484 [42] Ge T, Cai C, Chen P, Min F, Zhang M-X. The characterization on organic sulfur occurrence in coking
485 coal and mechanism of microwave action on thiophene. *Spectroscopy and Spectral Analysis*
486 2020;40(4):1321-7. [https://doi.org/10.3964/j.issn.1000-0593\(2020\)04-1321-07](https://doi.org/10.3964/j.issn.1000-0593(2020)04-1321-07).
- 487 [43] Ge T, Deng N, Min F. The dielectric properties of thiophene model compounds: insights for
488 microwave desulfurization of coking coal. *Energy Fuels* 2020;34(11):14101-8.
489 <https://doi.org/10.1021/acs.energyfuels.0c03001>
- 490 [44] Quan B, Liang XH, Ji GB, Cheng Y, Liu W, Ma JN, et al. Dielectric polarization in electromagnetic
491 wave absorption: Review and perspective. *J ALLOY COMPD* 2017;728:1065-75.
492 <https://doi.org/10.1016/j.jallcom.2017.09.082>.
- 493 [45] Ge T, Li F, Li Y. Influence of dielectric property of organic sulfur compounds on coal microwave
494 desulfurization. *ASIA-PAC J CHEM ENG* 2020. <https://doi.org/10.1002/apj.2581>.
- 495 [46] Sutton WH. Microwave processing of ceramic materials. *Am Ceram Soc Bull* 1989;68(2):376-86.
- 496 [47] Ge T, Zhang M. Dielectric properties of the model compounds of thiophene sulfur in coals and its
497 relation to molecular polarity. *Journal of China University of Mining and Technology*
498 2016;45(6):1245-50.
- 499 [48] Peng ZW, Hwang JY, Mouris J, Hutcheon R, Huang XD. Microwave penetration depth in materials
500 with non-zero magnetic susceptibility. *ISIJ Int* 2010;50(11):1590-6.

501 <https://doi.org/10.2355/isijinternational.50.1590>.

502 [49]Peng ZW, Lin XL, Li ZZ, Hwang JY, Kim BG, Zhang YB, et al. Dielectric characterization of

503 Indonesian low-rank coal for microwave processing. *Fuel Process Technol* 2017;156:171-7.

504 <https://doi.org/10.1016/j.fuproc.2016.11.001>.